Orbital Debris
Quarterly News
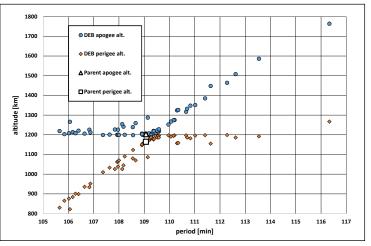
Inside...

Three Recent Breakup Events

This reportage begins with the 52nd fragmentation of a SOZ (*Sistema Obespecheniya Zapuska*) ullage motor, or SL-12 auxiliary motor, in late December 2019. Due to difficulties associated with characterizing this event, the breakup time has been estimated to be between 21 and 23 December. Notification of this event was provided after the ODQN's issue 24-1 was in production.
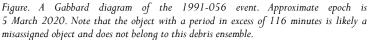
Ullage motors, used to provide three-axis control to the SL-12's Block DM fourth stage during coast and to settle propellants prior to an engine restart, were routinely ejected after the Block DM stage ignited for the final time. The reader is referred to a prior ODQN (ODQN, vol. 18, issue 4, pp. 12) for an illustration and engineering drawing of a typical SOZ unit. A total of 380 SL-12 auxiliary motors were cataloged between 1970 and 2012, of which 64 remain on orbit as of 5 March 2020. Of these 64, 32 are believed to be intact. The remaining 32 are known to have fragmented and remain on-orbit while an additional 20 fragmented parent bodies are no longer on-orbit.

This SOZ unit (International Designator 2009-070F, U.S. Strategic Command [USSTRATCOM] Space Surveillance Network [SSN] catalog number 36116), is associated with the launch of the Cosmos 2456-2458 spacecraft triplet, members of the Russian global positioning navigation system (GLONASS) constellation. The motor was in a highly elliptical 18980 × 512 km-altitude orbit at an inclination of 64.7° at the time of the breakup. Twenty-five pieces were observed; however, in addition to the parent body, only seven additional debris objects (piece

tags M-T, inclusive) have entered the satellite catalog as of 5 March 2020. Cause is assessed as a propulsion-related design flaw [1], in the context of long-term presence on-orbit—in this case, just over a decade. Due to difficulties in tracking objects in deep space elliptical orbits, this event may have produced a larger fragmentation debris ensemble than has been observed to date.

The second recent event was that of the Cosmos 2535 spacecraft (International Designator 2019-039A, SSN# 44421), which fragmented at approximately 22:00 GMT on 9 January 2020 after 1/2-year on orbit. Cosmos 2535 was launched aboard a Soyuz 2.1v rocket with Cosmos 2536-2538; two of these Cosmos spacecraft, including Cosmos 2535, were active and displayed a significant maneuver capability, while two did not maneuver. In addition to the Cosmos 2535 payload, a total of 17 additional debris (piece tags Q-AG inclusive) is associated with

Figure. A Gabbard diagram of the 1991-056 event. Approximate epoch is 5 March 2020. Note that the object with a period in excess of 116 minutes is likely a misassigned object and does not belong to this debris ensemble.

Recent Breakups

the 9 January event as of 5 March 2020.

At the time of the event, Cosmos 2535 was in a 645 x 607 km-altitude, 97.9° inclination orbit. There is little, if any, general information available as to the physical configuration, mass, and stored energy inventory of the spacecraft, excepting the presence of fuel/pressure systems and attitude control inferred from its extensive maneuver history. The cause of this event is presently unknown.

The third and most recent breakup was of an SL-14/*Tsyklon* 3 upper stage (International Designator 1991-056B, SSN# 21656); the S5M third stage fragmented at 10:46 GMT on 12 February 2020, after over 28 years on-orbit. At the time of the event the stage was in a 1206 x 1186 km-altitude, 82.56° inclination orbit. In addition to the parent body, 61 debris (piece tags C-BQ inclusive) has entered the satellite catalog as of 5 March 2020. These are depicted in the figure.

The 1.4 metric ton (dry) S5M stage uses storable hypergolic fuel, unsymmetrical dimethyl hydrazine, and a nitrogen tetroxide oxidizer. Five Tsyklon third stages have previously fragmented up to two decades after launch (Cosmos 1703 rocket body; International Designator 1985-108B, SSN# 8751), resulting in a total of 266 cataloged debris [2]. Those events were attributed to propulsion, likely caused by residual hypergolic propellants. The cause of this event, however, is unknown.

References

1. Chernyavskiy, G.M, Johnson, N.L., and McKnight, D.S. "Identification and Resolution of an Orbital Debris Problem with the Proton Launch Vehicle," Proceedings of the First European Conference on Space Debris, ESA SD-01, pp. 575-580, (July 1993).

2. Anz-Meador, P., Opiela, J., Shoots, D., *et al*. History of On-Orbit Satellite Fragmentations, 15th ed., NASA TM-2018-220037, (Nov. 2018). ♦

PROJECT REVIEW

The New NASA Orbital Debris Engineering Model 3.1

A. MANIS, M. MATNEY, P. ANZ-MEADOR, D. GATES, T. KENNEDY, J. SEAGO, A. VAVRIN, AND Y.-L. XU

The NASA Orbital Debris Program Office (ODPO) has developed the Orbital Debris Engineering Model (ORDEM) primarily as a tool for upper stage and spacecraft owners and operators and other users to understand the long-term risk of collisions with orbital debris. The newest version, ORDEM 3.1, incorporates the most recent high-fidelity datasets available to build and validate representative orbital debris populations encompassing low Earth orbit (LEO) to geosynchronous Earth orbit (GEO) altitudes for the years 2016-2050. In addition, newly developed data analysis techniques were applied to both new and legacy data to improve the assessment of orbital debris populations. A brief overview of the model updates is presented here; additional details can be found in [1].

The ODPO began development of orbital debris engineering models in the mid-1980s in support of the NASA Space Station Program Office. ORDEM 3.0 (see Orbital Debris Quarterly News [ODQN] vol. 18, issue 1, pp. 5-8) represented a significant upgrade in terms of model features and capabilities by extending the model to the GEO region; including uncertainties on the reported orbital debris flux; and most significantly, including a distribution in material density of orbital debris fluxes to better assess the risk to upper stages and spacecraft from different families of debris. ORDEM 3.1 maintains the same model architecture as ORDEM 3.0, while updating the model populations using newer data and selected analytical improvements.

ORDEM 3.1 Model Debris Populations

ORDEM is data-driven. The fundamental dataset for ODPO modeling efforts is the ODPO-maintained space traffic database, which is largely based upon the Space Surveillance Network (SSN) catalog. The yearly space traffic is propagated forward in time using the NASA LEO-to-GEO Environment Debris (LEGEND) model. The historical LEGEND component for ORDEM 3.1 covered launches from 1957 to 2015; the future projection covered years 2016 to 2050 and assumed a repeat of the previous 8-year launch traffic cycle with a post-mission disposal success rate of 90% for future rocket bodies and spacecraft. Fragments down to 1 mm in size from confirmed historical fragmentation events and statistically-modeled future collisions and explosions were created using a special version of the NASA Standard Satellite Breakup Model (SSBM), which extends the standard model to incorporate material density assignments (high, medium, and low) for fragments less than 10 cm. The initial LEO millimeter- to centimeter-sized populations modeled by LEGEND were scaled using data from the Haystack Ultrawideband Satellite Imaging Radar (HUSIR) collected with staring directions of 75° elevation, due East (referred to as "75E") and 20° elevation, due South (referred to as "20S").

Several special populations in LEO were modeled and scaled independently based on comparisons to the HUSIR data. These special populations include 10 breakup events with empirically customized fragment clouds; the major breakup fragment clouds from the 2007 Fengyun-1C (FY-1C) antisatellite test and the 2009 Iridium 33/Cosmos 2251 accidental collision; debris from shedding events by the SNAPSHOT vehicle and Transit-class spacecraft; and NaK reactor coolant droplets. The major breakups of FY-1C, Iridium 33, and Cosmos 2251 were reanalyzed for ORDEM 3.1 and the model results were compared to Haystack data from special observation campaigns around the time of each event to determine the initial state of these breakup fragment clouds. These comparisons indicated the need for an overall scaling of the number of fragments as well as incorporating the observed momentum transfer effects in the modeling of these major fragment clouds.

In addition, comparisons were made to the HUSIR calendar year (CY) 2013-2015 data, which represent the state of the fragment clouds after nearly a full solar cycle. This analysis showed that the fragments for these clouds, in particular Iridium 33, appeared to be decaying at a faster rate than predicted by the models, and enhancements were made to the area-to-mass ratios of debris in these clouds to capture this behavior. The NaK model was revised for ORDEM 3.1 to be in steady state. This was based on analysis of the most recent HUSIR data, along with a new screening method for NaK droplets, which suggested there is still a significant contribution of small (< 1 cm) droplets at the highest altitudes, where atmospheric drag should have removed them by now.

Data for debris smaller than 1 mm in LEO is provided by the database of impact features on the U.S. Space Transportation System (STS) orbiter

ORDEM 3.1

vehicle (*i.e.*, the space shuttle), as archived by NASA's Hypervelocity Impact Technology (HVIT) group. The database contains information on impact features to the shuttle, categorized by mission and surface. Data on craters in the shuttle windows (excluding the cargo bay windows) and radiator perforations was used for scaling a special small-particle degradation model. This model simulates the creation of millimeter-sized and smaller particles from large intact objects through a surface degradation process. For ORDEM 3.1, data from each STS mission and each window and radiator element was fitted independently to better preserve altitude and directionality effects.

For the GEO region, the population of objects smaller than the SSN catalog threshold was characterized using data from the Michigan Orbital DEbris Survey Telescope (MODEST). MODEST detections include objects correlated to those in the SSN catalog, termed correlated targets (CTs), as well as uncorrelated targets (UCTs), which may be either debris or intact objects. Several new analysis techniques were employed in building the GEO component of ORDEM 3.1, including a filter to extract objects most likely to be GEO fragmentation debris and a new approach to assign non-circular orbits to the fragmentation debris observed by MODEST.

Table 1 summarizes the ground-based and *in situ* datasets used for building and validating the ORDEM 3.1 model, including CY range of measurements and limiting sizes.

Table 1. Datasets Used for Building and Validating the ORDEM 3.1 Model Population

Data Source	Source Type	Orbit Region	Detection Size Range (approximate)	Calendar Year(s): Model Build	Calendar Year(s): Model Validation
STS windows, excluding cargo bay windows	*in situ*	LEO	$10 - 300\ \mu m$	1995-2011	N/A
STS radiators	*in situ*	LEO	$300\ \mu m - 1\ mm$	1995-2011	N/A
Hubble Space Telescope (HST) Bay 5 multilayer insulation (MLI)	*in situ*	LEO	$10 - 300\ \mu m$	N/A	1990-2009
HST Wide Field Planetary Camera-2 (WFPC-2) radiator	*in situ*	LEO	$50 - 300\ \mu m$	N/A	1993-2009
HUSIR, 75E staring	Radar	LEO	>5.5 mm	2007*, 2009*, 2013-2015	2016-2017
HUSIR, 20S staring	Radar	LEO	>2 cm	2015	N/A
Goldstone	Radar	LEO	$3 - 8\ mm$	N/A	2016-2017
SSN	Radar, Optical	LEO, GEO	>10 cm (LEO), >1 m (GEO)	1957-2015	N/A
MODEST (UCTs and CT debris)	Optical	GEO	>30 cm	2004-2009	2013-2014

Model Validation

A significant effort was made to validate ORDEM 3.1 using an independent set of data sources (see Table 1) to ensure the model provides a valid representation of the orbital debris environment. Typically, these observations come from the same sensor that provided data used for building the model, but for later years, to ensure that model predictions remain applicable in an evolving and dynamic orbital debris environment. In other cases, additional data sources provide a unique perspective on the environment that may extend the size of the orbital debris observation or contain more information about a particular orbital regime than was available from the source(s) used for building the model.

For LEO, HUSIR 75E data from 2016-2017 was used for validation of the > 5.5 mm populations. In addition, Goldstone radar data from 2016-2017 was used to validate the model populations at sizes smaller than the HUSIR threshold (down to approximately 3 mm for altitudes below 750 km). Sample validation results for cumulative surface area flux as a function of size for the altitude range from 400 km to 1000 km in 2016 are shown in Figure 1 for HUSIR 75E (A) and Goldstone (B). The roll-off

in sensitivity for HUSIR at approximately 5.5 mm at 1000 km is seen in the level-off of the data curve at small sizes in Figure 1 (A). Goldstone is more sensitive to the smaller debris particles than HUSIR, and the data is well-matched to the model prediction down to approximately 4 mm at 400 km to 1000 km. The uncertainties on the data are the one-σ uncertainties for counts from a Poisson distribution. The ORDEM 3.0 prediction also is shown for reference. The ORDEM 3.0 results represent a prediction of over a decade into the "future" relative to the years covered by the radar data used for building ORDEM 3.0. Thus ORDEM 3.1, which was built from datasets that are more recent, is expected to agree better with the newer data.

The sub-millimeter model populations were validated using recently-available data from impacts to the HST, specifically the MLI cover on the Bay 5 electronics box and the WFPC-2 radiator. Impacts to the Bay 5 MLI were analyzed to determine feature sizes and resulting projectile sizes based on newly-developed damage equations. New techniques to analyze craters on the WFPC-2 radiator using Scanning Electron Microscopy-Electron Dispersive X-ray analysis were also developed, which contributed data on sub-millimeter impacts at HST altitudes. Validation of a total micrometeoroid and orbital debris environment (ORDEM 3.1 plus the meteoroid flux from the NASA Meteoroid Engineering Model Release 2.0 [MEM R2]) against these datasets is shown in Figure 2. Uncertainties in the flux are the one-σ Poisson uncertainties, as for the radar data. The model is considered in excellent agreement with these datasets.
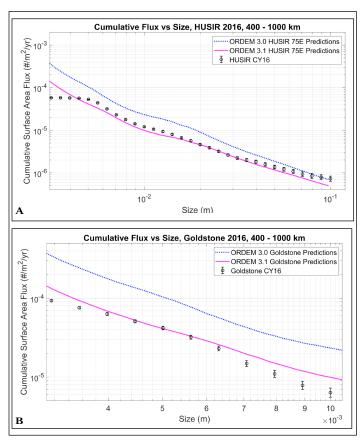
Figure 1. Comparison of the surface area flux vs estimated size between ORDEM 3.0, ORDEM 3.1, and measurements from HUSIR 75E (A) and Goldstone 75E (B) in CY 2016. The altitude is restricted from 400 km to 1000 km.
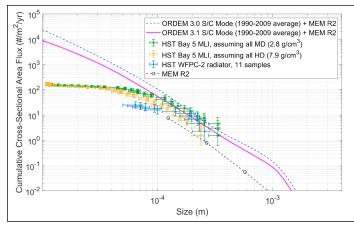
ORDEM 3.1

Figure 2. Comparison of the cumulative cross-sectional area flux vs size between ORDEM 3.0, ORDEM 3.1, and impact data from the HST Bay 5 MLI and WFPC-2 radiator. The ORDEM curves include the meteoroid flux estimates from the MEM R2 model. Two sets of MLI data points are shown, assuming all points as either medium density (MD) or high density (HD). The MEM R2 model results are also shown for reference.
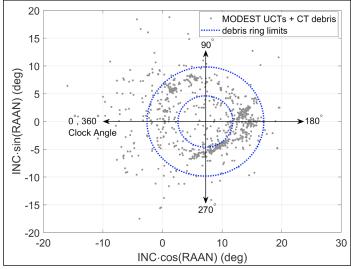

Figure 3. MODEST UCTs and CT debris, projected in (INC·cos(RAAN), INC·sin(RAAN)) Cartesian space, overlaid with the limits of the debris ring filter used to extract objects from within the ring that are most likely to be GEO fragmentation debris. The clock angle coordinate frame is also shown, with origin at (7.2°,0°); distributions in clock angle were used for comparison of the model GEO population to the MODEST validation data, as shown in Figure 4.

The GEO component of ORDEM 3.1 was validated against a MODEST dataset covering 2013-2014. Initial validation indicated discrepancies between the model and the MODEST 2013-2014 data in terms of "clock angle," defined as an angle in the Cartesian coordinates of (INC·cos(RAAN), INC·sin(RAAN)) where INC and RAAN are the orbit's inclination and right ascension of ascending node, respectively. In these coordinates, the path traced out during the precession cycle is a loop. The clock angle origin is defined by a vector originating at (7.2°,0°) and pointing toward the negative INC·cos(RAAN) direction, and the angle increases in a clockwise direction (see Figure 3). This clock angle is analogous to the "age" of orbits as they evolve away from 0° inclination under luni-solar perturbations. Two simulated breakups, potentially corresponding to unidentified breakups that occurred during the 2009-2013 break between

the MODEST observation campaigns, were added to the model to better match the MODEST 2013-2014 dataset. Figure 4 shows the distribution in clock angle for the initial (without the simulated breakups) and final (including the two simulated breakups) ORDEM 3.1 GEO population, as compared to the MODEST 2013-2014 data. Uncertainties shown for the MODEST data points are the one-σ confidence intervals from the standard Poisson counting error. Clearly, the final ORDEM 3.1 model is improved by the addition of the simulated breakups and is a good match to the MODEST data.

An Application of ORDEM 3.1

The HVIT team performed a series of risk assessment calculations comparing ORDEM 3.1 to ORDEM 3.0 for the International Space Station (ISS), ISS extra-vehicular activity, the Joint Polar Satellite System, and the Artemis 1 Interim Cryogenic Propulsion Stage. In all cases the ORDEM 3.1 risk, calculated as the mean number of failures, was reduced relative to ORDEM 3.0. In particular, the initial risk assessments indicate that OD risks decrease for ISS and Artemis by 8% and 24%, respectively, depending on the mission and/or element. This is consistent with the validation results shown in Figure 2, where the ORDEM 3.1 fluxes are lower than those of ORDEM 3.0.

Summary

The newest version of the NASA ODPO Orbital Debris Engineering Model, ORDEM 3.1, is now publicly available (https://software.nasa.gov/software/MSC-25457-1). Improved data analysis techniques applied during the population build phase of ORDEM 3.1 include new assessments of major breakup events (FY-1C antisatellite test and Iridium 33/Cosmos 2251 accidental collision) to account for momentum transfer effects and higher-than-expected drag rates; incorporation of directional and altitude influences in the STS window and radiator impact dataset; and a refined analysis of GEO debris objects and orbit definitions. As compared to ORDEM 3.0 predictions, ORDEM 3.1 provides significantly better fits to modern data and a more current representation of a dynamic orbital debris environment. When compared to ORDEM 3.0, in general, ORDEM 3.1 results in lower risk assessments for the missions analyzed to-date.

Reference

1. Matney, M., *et al*. "The NASA Orbital Debris Engineering Model 3.1: Development, Verification, and Validation," Paper presented at the 1st International Orbital Debris Conference, Sugar Land, TX, 9-12 December 2019. ♦
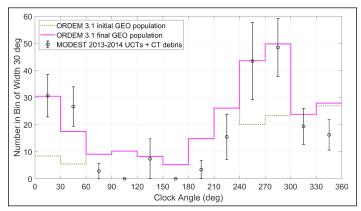

Figure 4. Clock angle distribution of the ORDEM 3.1 initial GEO population, final GEO population including the addition of two simulated breakups, and MODEST 2013-2014 UCTs and CT debris, for sizes from 30 cm to 1 m.
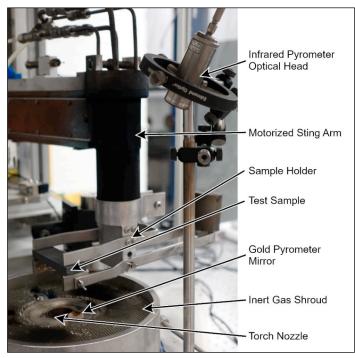
Composite Material Char Rate and Strength Retention Study at University of Texas at Austin

B. GREENE

One of the many responsibilities of the NASA Orbital Debris Program Office (ODPO) is to maintain tools to assess the number and size of spacecraft or upper stage fragments likely to survive atmospheric reentry, whether natural or targeted, and to calculate a casualty risk associated with the reentry of the structure. As part of efforts to improve the accuracy of these tools, a series of test campaigns have been carried out at the Inductively Coupled Plasma (ICP) Torch Facility at the University of Texas at Austin to investigate the demisability of fiber-reinforced plastic (FRP) materials. This has been a recent focus in the orbital debris community as previous assumptions about the demise of FRPs have proven inadequate [1-3]. Lips, *et al.*, for example, found that while several reentry risk assessment tools predicted the complete and rapid demise of a carbon-overwrapped aluminum pressure vessel, arc-jet testing found that, in fact, the carbon overwrap remained on the part and acted as a thermal shield, protecting the part from demise [1].

The first campaign carried out in April 2018 determined mass loss rates and material demise conditions of glass fiber-reinforced plastic (GFRP), carbon fiber-reinforced plastic (CFRP), and Kevlar. These results were presented at the 10th International Association for the Advancement of Space Safety (IAASS) conference in May 2019 [3].

The ODPO carried out a follow-up test campaign in August 2019 to investigate the charring rate and strength retention of the charred material for commonly used FRP composites like G-10 (a common glass fiber composite in circuit boards) and CFRP with various polymer matrices. Because the ICP facility operates in a shirt-sleeve environment, test samples can be changed within seconds or minutes, allowing a large number of samples to be tested in a short period. To facilitate even more rapid sample change, a custom sample holder, shown in Figure 1, was built, which clamped a rectangular sample using a pair of counterweighted jaws. The design of the jaws allowed a constant 4-point bending load to be applied to the sample by simply changing the offset of the upper arms with respect to the lower ones.

Two hundred and forty sample coupons were tested in this campaign, including samples of each of the following materials:

- DragonPlate EconomyPlate™ epoxy resin, carbon-fiber composite panel
- DragonPlate High-Temperature Pre-Preg* sheets (*proprietary, high-temperature, phenolic resin system)
- Wet layup, twill weave, vinyl ester resin CFRP panel
- Wet layup, twill weave, epoxy resin CFRP panel
- Wet layup 0/90, unidirectional, cyanate ester resin CFRP panel
- Wet layup 0/90, unidirectional, phenolic resin CFRP panel
- G10 epoxy/fiberglass panel

Three separate tests were performed to investigate different aspects of the demise model: (1) a charring and ablation rate test; (2) a post-reentry, charred material, strength retention test; and (3) an in-situ, charred material, strength retention test. Each test was performed for several materials at four different ICP conditions. The four flow conditions used in the test campaign are as follows:

1. Inert gas (argon) at a stagnation point heat flux of $20\,W/cm^2$
2. Oxidizing gas (2% air, 98% argon) at a stagnation point heat flux of $20\,W/cm^2$
3. Inert gas (argon) at a stagnation point heat flux of $30\,W/cm^2$
4. Oxidizing gas (2% air, 98% argon) at a stagnation point heat flux of $30\,W/cm^2$

The charring and ablation rate tests were designed to determine the rate of char penetration into a sample of composite material and, together with thermal gravimetric analysis (TGA) of each material, to estimate the rate of density change as the char layer penetrates the material depth. Two off-the-shelf materials—G10 and DragonPlate Economy Plate carbon fiber/epoxy resin composite panel—were exposed to all four test conditions for four different lengths of time: 5, 10, 40, and 80 seconds. A photograph of one of the char samples under test is shown in Figure 2. Select samples also were exposed to the plasma for up to 3 minutes. A carbon fiber/cyanate ester resin composite and a carbon fiber/phenolic resin composite also were tested at the low heat flux oxidizing gas condition (#2) only, due to limited supply of the material. During each test, the stagnation point and backside temperature of the sample was monitored using infrared thermometry.

Photographs of a G10 sample exposed to plasma for 80 seconds and a DragonPlate carbon fiber sample exposed to plasma for only 40 seconds are shown in Figure 3. Significantly more delamination was observed in the fiberglass samples since the thermal input melted the fibers in the laminate sheets. The char depth on a representative set of samples will be determined using x-ray computed tomography. Then, all test samples will be potted in epoxy and cross-sectioned for microscopy analysis.

The other two tests, post-reentry and *in situ*, were designed to investigate the residual strength of the material over various lengths of exposure time to reentry conditions, both during and after heating. In the Phase I tests, samples that had not completely demised regained some residual strength as they cooled. It is important to characterize the strength of the material during and after heating because the maximum

Figure 1. Test setup.

Infrared Pyrometer Optical Head

Motorized Sting Arm

Sample Holder

Test Sample

Gold Pyrometer Mirror

Inert Gas Shroud

Torch Nozzle

Composite Char Rate
continued from page 5

Figure 2. Sample under test. Credit: Colin Ye, University of Texas.
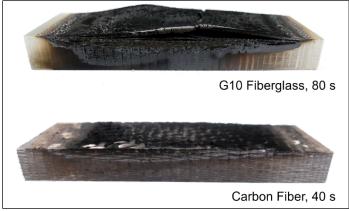

G10 Fiberglass, 80 s

Carbon Fiber, 40 s

Figure 3. Charred test samples of G10 fiberglass and carbon fiber.
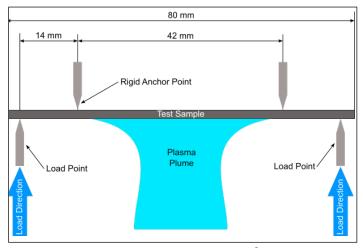

Figure 4. Four-point bend, in-situ, material strength test configuration.

aerodynamic stress is typically encountered at a lower altitude than the peak heat load, once the material has begun to cool.

The post-reentry char material strength retention test exposed 1- to 2-mm thick coupons to 5, 10, and 15 seconds of each flow condition and in a separate, upcoming test, these coupons will be loaded to mechanical failure to determine the residual strength in the cooled char material. Similar tests have been done at a heat flux between 1 and 5 W/cm² to study the susceptibility of FRPs to fire damage [4-5]. However, the heat flux of a natural decay reentry can be an order of magnitude greater.

The *in situ*, strength-retention test investigated the strength of the material at the elevated temperature of reentry. Similar tests also have been done at lower heat fluxes to study the effect of fire on structural composites [6]. In the current test, we exposed the same size coupons to a constant 4-point bending load, diagrammed in Figure 4, during plasma exposure, and measured (1) the time to mechanical failure and (2) the change in centerline deflection under load as a function of plasma exposure time. To apply the 4-point load, a new upper jaw was installed in the sample holder pictured in Figure 1 with jaws offset from the lower jaws by 14 mm. To keep the upper jaws from overheating due to increased proximity to the plasma, the jaws were encased in LI-2200 insulating tile material. The counterweight ensured a constant load throughout the travel distance of the lower jaw. During the test, the stagnation point and backside temperatures were monitored with infrared thermometry, and a video camera monitored the deflection of the sample under load. After the test, image processing was used to measure the deflection of the sample between the two inner load points of the 4-point bend jig.

Accurate char rate, thermal properties, and thermogravimetric data for the materials tested will aid in development of a charring/ablation model for structural composites to replace the melting/shredding assumption currently used. Measured strengths during and after peak heating of the material will help develop a reentry breakup model to more accurately reflect the mechanical behavior of structural materials during destructive reentry. The addition of these models will greatly improve the accuracy of the reentry risk analysis tools maintained by the ODPO.

References
1. Lips, T., *et al.* "About the Demisability of Propellant Tanks During Atmospheric Re-Entry from LEO." Paper presented at the 8th IAASS Conference, Melbourne, FL, USA, (2016).
2. Pagan, A., *et al.* "Experimental Thermal Response and Demisability Investigations on Five Aerospace Structure materials Under Simulated Destructive Re-Entry Conditions," 46th AIAA Thermophysics Conference, Washington, D. C, (June 2016).
3. Greene, B. R. and Sanchez, C. "Demisability of GFRP and CFRP Components of Reentering Orbital Debris: Phase I Test Results" 10th International Association for the Advancement of Space Safety Conference, El Segundo, CA, (2019).
4. Mouritz, A. "Post-Fire Flexural Properties of Fibre-Reinforced Polyester, Epoxy and Phenolic Composites," Journal of Materials Science, vol. 37, issue 7, pp. 1377-1386, (2002).
5. McKinnon, M., et al, "Pyrolysis Model for a Carbon Fiber/ Epoxy Structural Aerospace Composite," Journal of Fire Sciences, vol. 35, issue 1, pp. 36-61, (2017).
6. Di Modica, P. "Modelling Fire Behaviour of Composite Materials," PhD diss., Newcastle University, 2016. ♦

CONFERENCE AND MEETING REPORTS

The 2nd IAA Conference on Space Situational Awareness, 14-16 January 2020, Arlington, Virginia, USA

The 2nd IAA Conference on Space Situational Awareness (ICSSA) was held 14-16 January 2020 in Arlington, Virginia, with 60 members of the international orbital debris and space situational awareness community. The conference consisted of nine technical sessions and four plenary sessions. Topics included resident-space object and near-Earth object sensing, controlled re-entry and landing, spacecraft control, tracking, and risk assessment and policy.

The conference included several keynotes on "Risks from Orbital Debris and Space Situational Awareness," "Implementing SPD-3: The Dynamic Roles of Industry and Interagency," "Space Environment Management: Just in Time Collision Avoidance (JCA) – A Review," and "Space Debris and International Environmental Law." In addition to the keynote address, the NASA Orbital Debris Program Office participated in the technical session on RSO/NEO Sensing with the presentation "Recent Radar Observations of the Sub-Centimeter Orbital Debris Environment," which summarized recent findings of the sub-centimeter orbital debris population as measured by the Haystack Ultrawideband Satellite Imaging and Goldstone radars. Final papers can be downloaded by selecting the "ICSSA 2017 & 2020 Conference Papers" link from the conference website at http://reg.conferences.dce.ufl.edu/ICSSA/1358 . ♦

The 8th Satellite End of Life and Sustainable Technologies Workshop, 22-23 January 2020, Paris, France

The 8th Satellite End of Life and Sustainable Technologies Workshop, hosted by the French space agency CNES at their headquarters in Paris, France, was held 22 and 23 January 2020. Members of the Orbital Debris Program Office, along with nearly 50 representatives from industry, academia, and space agencies from around the world, were in attendance. The workshop opened with an introduction from the Inspector General of CNES, followed by a session on historical compliance with postmission disposal requirements and designing compliance into space systems.

Following the morning session were two sessions on postmission disposal of low Earth orbit (LEO) and geosynchronous Earth orbit (GEO) spacecraft. The GEO session featured presentations from Airbus, Eutelsat, and EUMETSAT on the disposal and passivation of their spacecraft using electric propulsion, including a special presentation from Airbus on the emergency disposal of a spacecraft using a Eurostar 2000+ bus following an anomaly. The LEO session had presentations on the disposal of the JASON-2, MetOp-A, and Myriade satellites. The MetOp-A spacecraft was designed before the adoption of space debris mitigation guidelines but planned to reenter in less than 25 years from the end of the mission, using several orbit lowering maneuvers. An anomaly in the summer of 2019 caused the residual fuel to decrease below the required amount for 25-year-rule compliance; engineers at EUMETSAT developed new options to reduce the fuel requirement below the amount left onboard. This technical ability and operational flexibility allow for a further two years of operations before the planned disposal in 2021.

Day two began with a session on the use of controlled reentry for postmission disposal. CNES presented on the planned controlled reentry of the Surface Water and Ocean Topography mission, a collaboration between CNES, NASA, the Canadian Space Agency, and the United Kingdom Space Agency, to be launched in 2022. The first session closed with a presentation by the ArianeGroup on the postmission disposal of upper stages for Ariane 6, which is expected to begin operations later this year.

The second session of day two included presentations on sustainable technologies and concepts; there were presentations by ESA and CNES on design-for-minimum-casualty-area and passivation technology development, as well as a presentation on how to remediate the orbital debris environment through alternative methods, such as last-minute collision avoidance maneuvers from external sources, or through improved state estimation of derelict objects. The NASA presentation on "Postmission Disposal Options in the 2019 USG Orbital Debris Mitigation Standard Practices (ODMSP)," was an overview of the updated disposal options available to satellite operators. Another presentation highlighted the balance between treaties, guidelines, regulation, and best practices for the sustainable use of space. The conference closed with a round-table discussion on how to guarantee space sustainability for future generations. More information can be found on the workshop website at http://eol-and-t4sc-workshop.evenium.net/ . ♦

Subscribe to the ODQN or Update Your Subscription Information

To be notified by email when a new issue of the ODQN is placed online, or to update your personal information, please navigate to the ODQN Subscription Request Form located on the NASA Orbital Debris Program Office (ODPO) website at https://orbitaldebris.jsc.nasa.gov/quarterly-news/subscription.cfm .

The ODPO respects your privacy. Your email address will only be used for communication from the ODQN Managing Editor.

CONFERENCE AND MEETING REPORTS – Cont.

The 2020 UN COPUOS STSC Meeting 3-14 February 2020, Vienna International Center, Vienna, Austria

The 57th session of the Scientific and Technical Subcommittee (STSC) of the United Nations (UN) Committee on the Peaceful Uses of Outer Space (COPUOS) took place at the Vienna International Center in Vienna on 3-14 February 2020. At the beginning of the session, Ms. Natália Archinard of Switzerland was elected to serve a 2-year term as the Chair of the Subcommittee, replacing the outgoing Chair, Ms. Pontsho Maruping of South Africa. In the new Chair's opening statement, Ms. Natália Archinard welcomed the Dominican Republic, Rwanda, and Singapore as the newest members of the Committee, bringing the total membership of COPUOS to 95 States.

Space debris was included as an agenda item again during the session. Many member States expressed concerns about the worsening orbital debris problem and the safety of future near-Earth space activities. Several technical presentations were provided under the agenda item. The United States' presentation was a summary of the 2019 update to the U.S. Government Orbital Debris Mitigation Standard Practices, as directed by the U.S. Space Policy Directive-3, the National Space Traffic Management Policy. The update covers all aspects of orbital debris mitigation and the updated elements are significant, meaningful, and achievable. It highlights the U.S. commitment to lead the global effort to mitigate the risk from orbital debris. France, as the 2019-2020 Chair of the Inter-Agency Space Debris Coordination Committee (IADC), provided an overview of the IADC's annual activities, which included a reentry prediction campaign, radar/optical measurements, long-term environment and active debris removal modeling, hypervelocity impact protection improvements, and updates to the IADC Space Debris Mitigation Guidelines. The European Space Agency also provided a summary of its space debris mitigation activities, including a post-mission-disposal compliance assessment of the global space missions. In low Earth orbit, when naturally compliant objects are excluded from the calculation, the level of compliance with the 25-year post-mission decay rule of upper stages and spacecraft has been, on average, less than 30% since 2000. Such a low level of compliance presents a serious challenge to the global community to manage the orbital debris problem. All STSC presentations are available at https://www.unoosa.org/oosa/en/ourwork/copuos/stsc/technical-presentations.html.

Following the successful adoption of the preamble and the 21 guidelines for the long-term sustainability of outer space activities (LTS) by the Committee in 2019, a decision was made to establish a new working group under a 5-year workplan and under the agenda item on the long-term sustainability of outer space activities of the Subcommittee. Preparation for this "LTS 2.0" working group was a major activity during the 57th session of the STSC. Multiple daily informal consultation meetings were held to discuss the structure of the working group leadership bureau, the four nominated chair candidates, and the priorities of the working group. No consensuses were reached by the Subcommittee at the end of the session. The LTS 2.0 preparation discussions will continue at the 63rd COPUOS session to be held in late 2020. ♦

DAS 3.0 NOTICE

Attention DAS Users: DAS 2.1.1 has been updated to DAS 3.0. DAS 3.0 is optimized for Microsoft Windows 7/8/10. Previous versions of DAS should no longer be used. NASA regulations require that a Software Usage Agreement must be obtained to acquire DAS 3.0. To begin the process, click on the **Request Now!** button in the NASA Software Catalog at https://software.nasa.gov/software/MSC-26690-1. An updated solar flux table can be downloaded for use with DAS 3.0.

UPCOMING MEETINGS

These events could be cancelled or rescheduled due to the COVID-19 pandemic. All information is current at the time of publication. Please consult the respective websites for updated schedule changes.

1-6 August 2020: 34th Annual Small Satellite Conference, Logan, UT, USA

Utah State University (USU) and the AIAA will sponsor the 34th Annual AIAA/USU Conference on Small Satellites at the university's Logan campus, Utah, USA. This year's theme is "Space Mission Architectures: Infinite Possibilities," and will explore the realm of space mission architectures and how these my support the diverse needs of the global space community. Conference information is available at the organizer's website at https://smallsat.org/. The abstract submission period closed on 4 February 2020.

UPCOMING MEETINGS – Continued

15-18 September 2020: 21st Advanced Maui Optical and Space Surveillance Technologies Conference, Maui, Hawaii, USA

The technical program of the 21st Advanced Maui Optical and Space Surveillance Technologies Conference (AMOS) is anticipated to focus on subjects that are mission critical to Space Situational Awareness. The technical sessions include papers and posters on Orbital Debris, Space Situational Awareness, Adaptive Optics & Imaging, Astrodynamics, Non-resolved Object Characterization, and related topics. The abstract submission deadline passed on 1 March 2020. Additional information about the conference is available at https://amostech.com and this announcement will be updated in the ODQN as details become available.

2 December 2020: 5th Space Debris Re-entry Workshop, Darmstadt, Germany

The European Space Operations Centre (ESOC) will host the 5th Space Debris Re-entry Workshop in December 2020. The workshop aims to address the side effects of the increased traffic to orbit which triggered a renewed interest in the practicalities of having objects, large and small, re-entering uncontrolled after the end of mission. The symposium style for the past events transitions this year to a workshop around the open problems burgeoning by the increase in uncontrolled re-entry "traffic": how to transition from uncertainty assessment to operational products when it comes to re-entry predictions and orbital lifetimes? Which multi-physics driven break-up processes produce predictions which can be verified on a macroscopic level to cause first fragmentation? The submission of abstracts on those questions is encouraged, but the venue is of course open to other topics related to general orbital lifetime estimation, re-entry predictions on catalogue level, low thermosphere orbit observations and orbit determination, material and aerothermal responses of re-entering objects in the continuum regime. Among the objectives of the workshop are linking space surveillance, astrodynamics, and re-entry physics to cover all aspects of the problem. The abstract and registration deadline dates are 12 October and 9 November 2020, respectively. Detailed information is available at https://reentry.esoc.esa.int/home/workshop .

14-16 December 2020: 6th International Workshop on Space Debris Modeling and Remediation, Paris, France
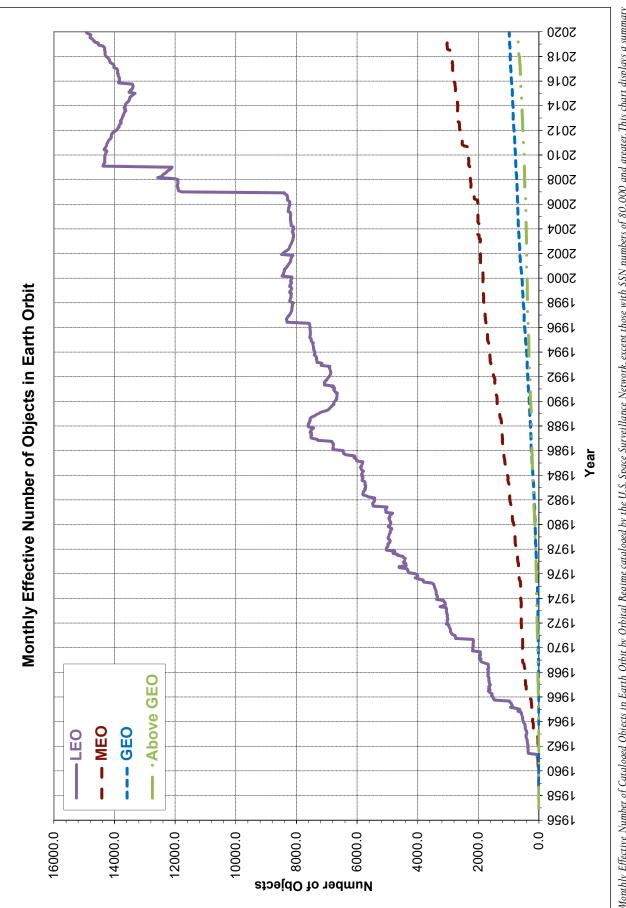
CNES Headquarters will host the 6th International Workshop on Space Debris Modeling and Remediation. Topics are anticipated to include, but are not necessarily limited to, modelling, including specificities coming from small satellites and constellations; high level actions, road-maps, associated to Debris Remediation; Remediation system studies, including those relative to small debris; Design of specific concepts, including new ideas relative to Just-in-time Collision Avoidance and proposals devoted to large constellations and small satellites; concepts derived from current Space Tugs initiatives; GNC aspects, rendezvous sensors and algorithms, de-spin, control during de-boost; and Policy, Economics, Insurance, Intellectual property, national security, and international cooperation aspects of Debris remediation. Workshop attendance is limited to 130. The abstract submission deadline is 14 September 2020, and additional details regarding the process are available from Mr. Christophe Bonnal at Christophe.bonnal@cnes.fr.

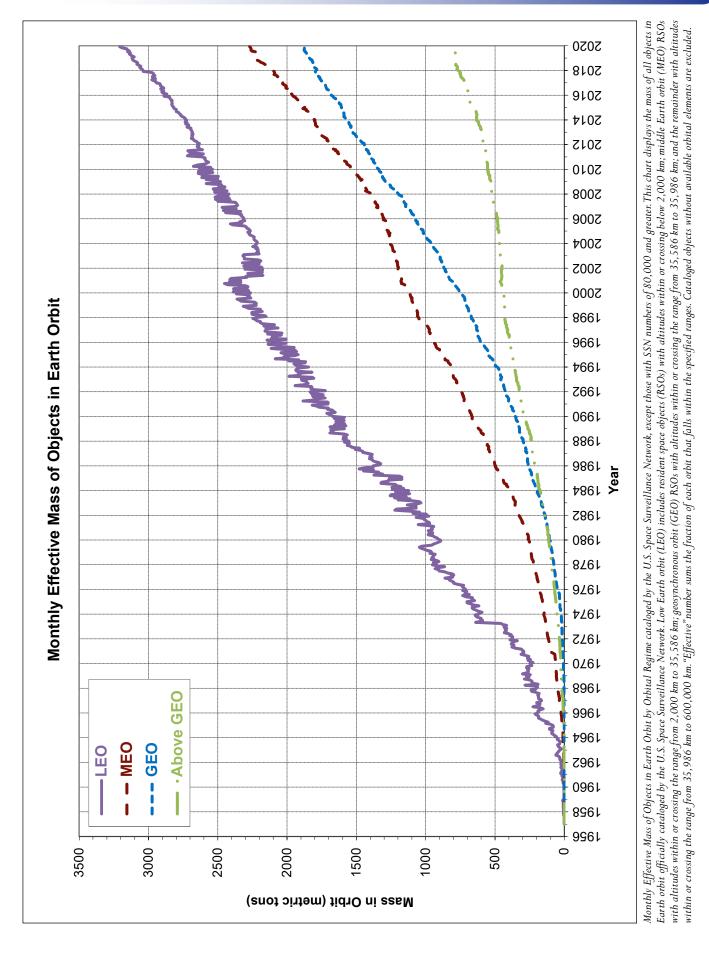### 28 January-4 February 2021: COSPAR 2021, Sydney, Australia

Due to the worldwide COVID-19 pandemic the 43rd Assembly of the Committee on Space Research (COSPAR) Scientific will convene in the Sydney International Convention Center in early 2021, rather than August 2020, as COSPAR 2021. The COSPAR panel Potentially Environmentally Detrimental Activities in Space (PEDAS) will conduct a program entitled "The Science of Human-Made Objects in Orbit: Space Debris and Sustainable Use of Space." PEDAS.1 sessions will include advances in ground- and space-based measurements of the orbital debris environment, micrometeoroid and orbital debris environment modeling, end-of-life concepts, and solutions to fundamental operational challenges. The abstract submission period closed on 14 February 2020. Please see the COSPAR PEDAS.1 session website at https://www.cospar-assembly.org/admin/session_cospar.php?session=953 and the assembly website https://www.cospar2020.org/ for further information.

26-28 October 2021: 11th International Association for the Advancement of Space Safety (IAASS) Conference, Osaka, Japan

The 11th conference of the IAASS, organized in concert with the Japan Aerospace Exploration Agency, has as its theme "Managing Risk in Space." Major debris-related topics include designing safety into space vehicles, space debris mitigation and remediation, re-entry safety, nuclear safety for space missions, safety risk management and probabilistic risk assessment, and launch and in-orbit collision risk. The conference's abstract submission deadline is on 30 April 2021. Additional information for the 2021 IAASS is available at http://iaassconference2021.space-safety.org/.

Monthly Effective Number of Objects in Earth Orbit

Number of Objects (y-axis)

Legend:
- LEO
- MEO
- GEO
- Above GEO

Year (x-axis)

Monthly Effective Number of Cataloged Objects in Earth Orbit by Orbital Regime cataloged by the U.S. Space Surveillance Network, except those with SSN numbers of 80,000 and greater. This chart displays a summary of all objects in Earth orbit officially cataloged by the U.S. Space Surveillance Network. Low Earth orbit (LEO) includes resident space objects (RSOs) with altitudes within or crossing below 2,000 km; middle Earth orbit (MEO) RSOs with altitudes within or crossing the range from 2,000 km to 35,586 km; geosynchronous orbit (GEO) RSOs with altitudes within or crossing the range from 35,586 km to 35,986 km; and the remainder with altitudes within or crossing the range from 35,986 km to 600,000 km. "Effective" number sums the fraction of each orbit that falls within the specified ranges. Cataloged objects without available orbital elements are excluded.

Monthly Effective Mass of Objects in Earth Orbit

Monthly Effective Mass of Objects in Earth Orbit by Orbital Regime cataloged by the U.S. Space Surveillance Network. This chart displays the mass of all objects in Earth orbit officially cataloged by the U.S. Space Surveillance Network. Low Earth orbit (LEO) includes resident space objects (RSOs) with altitudes within or crossing below 2,000 km; middle Earth orbit (MEO) RSOs with altitudes within or crossing the range from 2,000 km to 35,586 km; geosynchronous orbit (GEO) RSOs with altitudes within or crossing the range from 35,586 km to 35,986 km; and the remainder with altitudes within or crossing the range from 35,986 km to 600,000 km. "Effective" number sums the fraction of each orbit that falls within the specified ranges. Cataloged objects without available orbital elements are excluded.

SATELLITE BOX SCORE

(as of 01 April 2020, cataloged by the U.S. SPACE SURVEILLANCE NETWORK)

Country/ Organization	Spacecraft*	Spent Rocket Bodies & Debris	Total
CHINA	395	3716	4111
CIS	1537	5251	6788
ESA	91	58	149
FRANCE	69	509	578
INDIA	100	125	225
JAPAN	185	113	298
USA	2215	4897	7112
OTHER	1053	123	1176
TOTAL	5645	14792	20437

* active and defunct

Visit the NASA

Orbital Debris Program Office Website

www.orbitaldebris.jsc.nasa.gov

Technical Editor
Phillip Anz-Meador, Ph.D.

Managing Editor
Debi Shoots

Correspondence can be sent to:

J.D. Harrington
j.d.harrington@nasa.gov

or to:

Noah Michelsohn
noah.j.michelsohn@nasa.gov

INTERNATIONAL SPACE MISSIONS

01 January – 29 February 2020

Intl.* Designator	Spacecraft	Country/ Organization	Perigee Alt. (KM)	Apogee Alt. (KM)	Incli. (DEG)	Addnl. SC	Earth Orbital R/B	Other Cat. Debris
1998-067	ISS dispensed payloads	various	409	423	51.6	8	0	3
2019-071	ISS Visiting Vehicle dispensed payloads	USA	455	476	51.6	14	0	0
2020-001A	STARLINK-1073	USA	548	551	53	59	0	4
2020-002A	TJS-5	CHINA	35784	35789	0.84	0	1	0
2020-003A	OBJECT A	TBD	476	493	97.32	0		
2020-003B	NUSAT-7 (SOPHIE)	ARGENTINA	474	493	97.32			
2020-003C	NUSAT-8 (MARIE)	ARGENTINA	476	493	97.33			
2020-003D	OBJECT D	TBD	474	493	97.32			
2020-003E	OBJECT E	TBD	480	496	97.21			
2020-003F	OBJECT F	TBD	477	488	97.36			
2020-003G	OBJECT G	TBD	462	491	97.29			
2020-003H	OBJECT H	TBD	429	491	97.44			
2020-004A	YINHE-1	CHINA	619	640	86.4	0	1	1
2020-005A	GSAT 30	INDIA	35806	35886	0.02	0	1	1
2020-005B	EUTELSAT KONNECT	EUTELSAT	EN ROUTE TO GEO					
2020-006A	STARLINK-1132	USA	417	419	53	59	0	4
2020-007A	USA 294	USA	NO INITIAL ELEMENTS			0	2	0
2020-008A	ONEWEB-0013	UK	524	554	87.52	33	0	0
2020-009A	IGS O-7	JAPAN	NO ELEMS. AVAILABLE			0	1	0
2020-010A	SOLAR ORBITER	UK	HELIOCENTRIC			0	0	0
2020-011A	CYGNUS NG-13	USA	416	423	51.65	0	1	1
2020-012A	STARLINK-1138	USA	544	546	53	59	1	4
2020-013A	JCSAT 17	JAPAN	EN ROUTE TO GEO			0	1	1
2020-013B	GEO-KOMPSAT-2B	SOUTH KOREA	35781	35793	0.04			
2020-014A	OBJECT A	CHINA	475	483	35.01	0		
2020-014B	OBJECT B	CHINA	475	483	35.01			
2020-014C	OBJECT C	CHINA	475	483	35.01			
2020-014D	OBJECT D	CHINA	474	482	35			
2020-014E	OBJECT E	CHINA	475	483	35.01			
2020-015A	MERIDIAN 9	RUSSIA	1063	39282	62.85	0	1	0

* Intl. = International; SC = Spacecraft; Alt. = Altitude; Incli. = Inclination; Addnl. = Additional; R/B = Rocket Bodies; Cat. = Cataloged

The NASA Orbital Debris Photo Gallery has added high resolution, computer-generated images of objects in Earth orbit that are currently being tracked. They may be downloaded. Full instructions are at the webpage:

https://orbitaldebris.jsc.nasa.gov/photo-gallery/